Endoneurial pathology of the needlestick-nerve-injury model of Complex Regional Pain Syndrome, including rats with and without pain behaviors

Published in final edited form as:
Eur J Pain. 2012 January ; 16(1): 28–37. doi:10.1016/j.ejpain.2011.05.004.

Endoneurial pathology of the needlestick-nerve-injury model of Complex Regional Pain Syndrome, including rats with and without pain behaviors

Max M. Klein, Ph.D.[*], **Jeung Woon Lee, Ph.D.**[*], **Sandra M. Siegel, Ph.D., D.V.M.**, **Heather M. Downs, B.S.**, and **Anne Louise Oaklander, M.D., Ph.D.**
Departments of Neurology and Pathology, Massachusetts General Hospital, Harvard Medical School, Boston, MA

Abstract

Current rodent models of neuropathic pain produce pain hypersensitivity in almost all lesioned animals and not all identified experimental effects are pain specific. 18G needlestick-nerve-injury (NNI) to one tibial nerve of outbred Sprague-Dawley rats models the phenotype of Complex Regional Pain Syndrome (CRPS), a post-traumatic neuropathic pain syndrome, leaving roughly half of NNI rats with hyperalgesia. We compared endoneurial data from these divergent endophenotypes searching for pathological changes specifically associated with pain-behaviors. Tibial, sural, and common sciatic nerves from 12 NNI rats plus 10 nerves from sham-operated controls were removed 14 days post-surgery for morphometric analysis. $PGP9.5^{+}$ unmyelinated-fibers were quantitated in plantar hindpaw skin. Distal tibial nerves of NNI rats had endoneurial edema, 30% fewer axons, twice as many mast cells, and thicker blood-vessel walls than uninjured tibial nerves. However the only significant difference between nerves from hyperalgesic versus non-hyperalgesic NNI rats was greater endoneurial edema in hyperalgesic rats ($p < 0.01$). We also discovered significant axonal losses in uninjured ipsilateral sural nerves of NNI rats, demonstrating spread of neuropathy to nearby nerves formerly thought spared. Tibial and sural nerves contralateral to NNI had significant changes in endoneurial bloodvessels. Similar pathological changes have been identified in CRPS-I patients. The current findings suggest that severity of endoneurial vasculopathy and inflammation may correlate better with neuropathic pain behaviors than degree of axonal loss. Spread of pathological changes to nearby ipsilateral and contralesional nerves might potentially contribute to extraterritorial pain in CRPS.

Keywords

Neuralgia; reflex sympathetic dystrophy; hyperalgesia; allodynia; dystonia; morphometry; mast cells

Corresponding author: Anne Louise Oaklander, M.D., Ph.D., Massachusetts General Hospital, 275 Charles St. /Warren Bldg. 310, Boston, MA 02114, Tel: 617-726-4656 Fax: 617-726-0473, aoaklander@partners.org.
[*]These authors contributed equally

This study does not concern commercial products and the authors have no conflicts of interest.

1. Introduction

Chronic pain is a rare complication of damage to pain-system neurons, most often to nociceptive axons in peripheral nerves or roots. These long axons are vulnerable to traumatic or metabolic disconnection from their distant cell bodies, which can cause distal Wallerian degeneration. This is well modeled by nerve transection (axotomy). Most axotomies do not cause chronic pain, but even small and seemingly trivial injuries that affect nociceptive axons occasionally cause chronic neuropathic pain (neuralgia) perceived in and around the injured axons' receptive fields. The neuralgia and/or complex regional pain syndrome (CRPS) that very rarely follows needle penetration of small sensory nerves, e.g., from phlebotomy, (Horowitz, 1994) is a bellwether syndrome that we have modeled in rats (Siegel et al., 2007).

Although rodent models have generated considerable molecular and pharmacological data about neuralgia, these have not translated well into new pain treatments (Lacroix-Fralish and Mogil, 2009). The efficiency of these models – almost all lesioned rats develop allodynia and/or hyperalgesia – might be one factor. Data from outlier rodents without hypersensitivity are often discarded or obscured in the summary statistics from groups of lesioned animals, making it difficult to determine whether the experimental effects are truly pain-associated or not. Our needlestick nerve injury (NNI) model (Siegel et al., 2007; Lee et al., 2009) attempts to address these concerns with a highly standardized small axotomy that produces variable phenotypes, presumably due to genetic diversity within the outbred Sprague-Dawley strain (Mogil et al., 1998). In addition to pain behaviors, NNI models several other CRPS features including distal-limb edema, and hindpaw postures that may model CRPS/dystonia (Siegel et al., 2007). Roughly half of NNI rats develop evoked pain-hypersensitivity interpreted as modeling neuralgia. The others have unchanged or increased sensory thresholds (hypoesthesia). These divergent endophenotypes cannot be adequately represented by summary statistics from groups of lesioned animals because mean values from a group that contains increased as well as reduced thresholds can erroneously seem unchanged. Reporting the prevalences of specific phenotypes or outcomes is more useful.

The NNI model aims for clinical relevance by lesioning a distal nerve-branch rather than a rarely injured proximal nerve-trunk. Cutting only some axons and part of the epineurium is also more clinically representational. Some preserved axons are required anyway for stimulus-evoked pain; total axotomy produces only sensory unresponsiveness (numbness) in autonomously innervated territories (Decosterd and Woolf, 2000). The NNI model avoids nerve ligation. Although common in pain-models (Bennett and Xie, 1988; Seltzer et al., 1990; Kim and Chung, 1992; Decosterd and Woolf, 2000) this is carefully avoided in medical practice. Retained juxtaneural suture can cause inflammation and hyperalgesia that is influenced by its composition and other factors (Basbaum et al., 1991; Maves et al., 1993).

Here we characterize the endoneurial pathology of 18G tibial-nerve NNI rats whose pain behaviors have previously been reported in aggregate. We studied blood vessels, and quantified inflammatory cells as well as surviving axons because all three tissue types are involved in CRPS. By identifying which changes are preferentially expressed among NNI rats with pain behaviors, we hope to identify more-specific biomarkers for neuralgia.

2. Design and Methods

Twelve young adult, male, Sprague-Dawley rats (200–250 g; Charles River Labs, Wilmington, MA) were studied using procedures approved by our Institutional Animal Care and Use Committee and conforming to ethical guidelines (Zimmermann, 1983). They were housed in small groups in smooth-floored cages and had free access to food and water. A

12-hour light/dark cycle was maintained with testing during the light phase. NNI surgery comprised exposure of the left common sciatic trifurcation in anesthetized rats (50 mg/kg intraperitoneal sodium pentobarbital, Abbott Labs, North Chicago, IL). The tibial branch was identified and penetrated once with a surgical needle held with the bevel perpendicular to the nerve axis. The muscles and skin were closed and rats recovered without medication. The rats whose pathological analyses are described here are a subset of a larger group of rats whose phenotypes were previously described in detail (Siegel et al., 2007). We chose the rats with 18G needlestick (1.28 mm outer diameter) nerve-injury for pathological study because the mean severity of epidermal neurite loss in the hindpaw after 18G NNI (31%) closely matches the mean severity of loss of epidermal nerve fibers (29%) reported for human CRPS-I patients (Oaklander et al., 2006). Five sham-operated male rats that were randomly chosen and handled identically provided controls. Sham-operation was performed on the left hind limb identically to NNI except that the epineurium was merely touched with a cotton swab before closing the surgical incision.

2.1 Testing plantar hindpaw sensory function

The tibial- and sural-innervated areas of the plantar surface of rats' ipsilesional (left) and contralesional (right) hindpaws were studied as previously reported (Siegel et al., 2007). Sensation was tested by stimulating the tibial- and sural-innervated sites through a wire-mesh floor on days 1, 3, 7, 10, and 14 post-operatively.

Static low-threshold mechanosensation was measured by stimulating rats' plantar hindpaws with a set of balance-calibrated von Frey monofilaments (Stoelting Co., Wood Dale, IL). The threshold for paw withdrawal was defined as the thinnest monofilament that produced withdrawal on at least two of five consecutive trials for two consecutive filaments (Anseloni et al., 2002). Punctate mechanical nociception was tested using a stopwatch to time the duration of hindpaw withdrawal after one safety-pin prick. The normal response was no withdrawal or a withdrawal too brief to time and hyperalgesia was defined as withdrawal duration ≥ 1s. Cold sensation was tested by syringe application of a drop of acetone to the lateral plantar hindpaw; duration of paw withdrawal was recorded by stopwatch. The normal response was no withdrawal or withdrawal too brief to time; abnormal was defined as withdrawal duration ≥ 1s.

2.2 Tissue collection and processing

After terminal pentobarbital anesthesia, a 2-mm skin punch was removed from each of the four hindpaw study sites, fixed in 2% periodate lysine paraformaldehyde, cut into 50 μm vertical sections and immunolabeled against PGP9.5 (Chemicon, Temecula, CA), a pan-axonal marker, using standard methods (Lauria et al., 2005). Quantitative data were obtained from the epidermis where axons individuate. Rats were then injected transcardially with 0.1 cc heparin and perfused with 200 ml 0.9% saline (4°C) followed by 200 ml of freshly prepared 4% paraformaldehyde, 0.13% para-picric acid in 0.1 M phosphate buffered saline (pH 7.4, 4°C). Nerves were dissected and post-fixed overnight in fresh 5% glutaraldehyde in Sorenson's buffer (4°C). Tibial-nerve samples whose proximal ends were 5 mm distal to the site of NNI were processed through graded alcohols, propylene oxide, and epoxy resin using a Leica Lynx tissue processor and standard methods. Nerves were oriented longitudinally and polymerized overnight in epoxy resin (60°C). One-μm transverse sections were cut by glass knife using a Leica UltracutR ultramicrotome, placed on coated microscope slides, stained with 1% borate-buffered toluidine blue, and coverslipped.

2.3 Data collection and analysis

All slides were masked and randomized prior to data collection. A single experienced morphometrist counted the number of PGP9.5+ neurites in the skin biopsy slides using a

Leica DMLS microscope and a 40× objective. The standard counting rules used for clinical diagnosis were applied (Lauria et al., 2005). Our laboratory reports neurite densities per mm^2 skin surface area rather than per linear mm to factor in section thickness. Data on endoneurial contents were collected from single nerve cross-sections. Some data were gathered at the microscope using a 40× objective (e.g. numbers of blood vessels). Smaller structures were measured digitally on enlarged photomicrograph montages captured using an Olympus DP25 camera and digitally assembled using Photoshop 7.0 (Adobe Systems, Inc., San Jose, CA). NIH ImageJ software (Rasband, W.S., ImageJ, U. S. National Institutes of Health, Bethesda, Maryland, USA, http://rsb.info.nih.gov/ij/, 1997–2009) was used to measure microvessel wall thicknesses and luminal areas and to count each myelinated axon in all fascicles of each nerve. The total area of all fascicles within each nerve was measured by digitally tracing along the outer boundary of each fascicle's contents inside the perineurium. Voids between the fascicular contents and the perineurium were excluded (Figure 1). All endoneurial blood vessels (microvessels) in all fascicles of each nerve were counted and then each microvessel's luminal area was measured by ImageJ from digital tracing along the inner endothelial surface. Microvessel wall-thickness was digitally measured perpendicular to the vessel wall at a representative location selected to avoid nuclear regions. Mast cells were identified as 20–30 μm diameter cells with basophilic and metachromatic granules that often obscure their uni-lobed nucleus. Electron microscopic examination confirmed the identity of mast cells in preliminary experiments (data not shown). In a secondary analysis to assess mast-cell activity, each mast cell was categorized as either granulated or degranulated (if ≥ 50% of the cytoplasm was eosinophilic and largely devoid of granules) (Taiwo et al., 2004).

2.4 Study design and analysis

The first analysis compares grouped data from all NNI nerves and all controls to characterize the endoneurial cellular pathology of 18G needlestick 14 days prior to analysis. Comparing left and right nerves from the 5 left-tibial sham-operated rats identified no significant differences therefore data from left and right control nerves were combined. One left sural nerve from a non-hyperalgesic rat was lost during processing. Among common sciatic nerves, 11/12 NNI and 5/10 control nerves were adequate and underwent morphometric analysis. 43/44 hindpaw skin-biopsies were adequate and one cross-section from each distal nerve stump was digitally photographed for morphometric analysis.

For the second analysis, data from individual rats were stratified into different groups for comparison based on the presence or absence of hypersensitivity in the receptive field at day 14 postoperatively. Stringent criteria were applied to select nerves from rats with and without pain behaviors for pathological comparison. Rats categorized as non-hyperalgesic were required to have no postoperative hyperalgesia or allodynia, specifically no reduction in thresholds for hindpaw withdrawal from von Frey filaments from baseline values, plus no prolonged withdrawal from pin or acetone. Because NNI caused persistent pin hyperalgesia and cold allodynia far less often than monofilament allodynia (Siegel et al., 2007), it was not feasible to require that abnormal pin and cold sensation be present in addition to mechanical allodynia to define a rat as hyperalgesic. The following inclusion criteria concerning mechanical allodynia were applied to define nerves of hyperalgesic rats: For ipsilesional nerves, day 14 von Frey thresholds at that nerve's receptive field had to be ≥ 70% reduced from baseline. For contralesional nerves, von Frey thresholds had to be ≥ 30% reduced from baseline.

Statistica 7.1 (StatSoft Inc., Tulsa, OK) software was used. Means ± standard errors summarize data from groups. Data from all NNI and control nerves were compared by 2-sided *t* tests for independent (orthogonal) groups. The need for correction for multiple comparisons was carefully considered. The goal of this study is not testing a unitary

hypothesis, and not all of the 7 primary outcome variables are expected to be correlated, so the need for correction is debatable. To be conservative, a Bonferroni correction was made using an estimated correlation of 0.5. This lowered α from 0.05 to 0.01889 for each test (for 7–20 degrees of freedom).

3. Results

3.1 Overall effects of 18G tibial-NNI on injured and uninjured nerves

Analysis of injured tibial nerve distal to NNI (Table 1) showed similar significant losses of myelinated axons as seen in the nerve cross-sections (−32%) and unmyelinated axons in the epidermis (−31%). There were also significant vascular and inflammatory changes, specifically intrafascicular edema, thickened blood-vessel walls, and a near doubling of mast cells. These mast cells were clearly visible, often near blood vessels. Importantly, tibial-NNI overtly affected nearby ipsilesional sural nerves, although these had not been penetrated by the needle (Figure 1, Table 2), producing statistically significant changes of similar magnitude to those detected within injured tibial nerves. These included 40% loss of epidermal neurites at the ipsilesional sural-innervated study site, 35% thicker blood-vessel walls and a trend towards fewer myelinated axons (−28%) as well. NNI also was associated with subtle effects on uninjured contralesional nerves. The only statistically significant change in tibial nerves (Table 1) was 14% thinner vessel-walls; there was a trend towards endoneurial edema. Sural nerves contralateral to tibial-NNI (Table 2) had significantly dilated blood-vessels (+85% intraluminal area), and a trend towards loss of epidermal neurites (−22%).

3.2 Characteristics of rats with versus without hindpaw hyperalgesia after NNI

When all 12 NNI rats were analyzed together as a group, the mean threshold for hindpaw withdrawal from monofilament stimulation at the ipsilateral tibial-innervated study site was reduced from a preoperative baseline of 1052 mN to 683 mN at day 14. Mean values from the ipsilateral sural-innervated site fell from a preoperative baseline of 1109 mN to 456 mN at day 14. But these mean values do not adequately represent the situation because post-NNI sensory responses actually ranged widely from baseline in opposite directions between severe allodynia through severe sensory loss/hypoesthesia. 5/12 hypersensitive rats had pin hyperalgesia at any study site and 2/12 had cold allodynia as well.

The division of rats into groups with or without tibial-zone hyperalgesia is summarized in Figure 2A. More specifically, ipsilesional tibial nerves from six NNI rats (6/12) were associated with hyperalgesic receptive fields. In the hyperalgesic group, the mean post-operative von Frey threshold for hindpaw withdrawal was reduced from 1148 mN to 168 mN. When each rat's baseline was normed to 100%, mean 14 days values were 15% of baseline; range = 5 – 30%). Five rats (5/12) were categorized as having non-hyperalgesic receptive fields; their mean von Frey thresholds changed from 811 mN to 1188 mN. When each rat's baseline was normed to 100%, mean 14 days values were 168% of baseline; range = unchanged – 247%).

Five contralesional tibial nerves met inclusion criteria for having hyperalgesic receptive fields; their mean threshold was reduced from 1337 mN to 498 mN. When each rat's baseline was normed to 100%, mean 14 days values were 38% of baseline (range = 68% – 9%). 6 met criteria for having non-hyperalgesic receptive fields; their mean threshold increased from 767 mN to 1024 mN. When each rat's baseline was normed to 100%, mean 14 days values were 140% of baseline (range = unchanged – 247%). One nerve from a rat with an intermediate ipsilesional tibial-site withdrawal threshold (74% of baseline) and one contralesional tibial nerve from a rat with an intermediate contralesional tibial-site

withdrawal threshold (74% of baseline) did not meet inclusion criteria for either hyperalgesia or non-hyperalgesia and thus were excluded from this second analysis.

The division of rats into groups with or without sural-zone hyperalgesia is summarized in Figure 2B. Among ipsilesional sural nerves, six met criteria for hyperalgesic receptive fields; their mean threshold was reduced from 1132 mN to 118 mN. When each rat's baseline was normed to 100%, mean 14 days values were reduced to 11% of baseline (range = 5% – 16%). Only 3 met criteria as non-hyperalgesic; two were unchanged and one increased to 422%. Seven contralesional sural nerves were categorized as having hyperalgesic receptive fields; their mean threshold was reduced from 1260 mN to 550 mN. When each rat's baseline was normed to 100%, mean 14 days values were reduced to 44% of baseline (range = 59% – 9%). 4 met criteria as non-hyperalgesic; three were unchanged and one was at 168% of baseline. Three nerves from rats with intermediate ipsilesional sural-site withdrawal thresholds (40 – 51% of baseline) and one contralesional sural nerve from an NNI rat with an intermediate sural-territory withdrawal threshold (74% of baseline) did not meet inclusion criteria for either hyperalgesia or non-hyperalgesia and thus were excluded from this analysis.

3.3 Comparison of endoneural pathology in hyperalgesic versus non-hyperalgesic NNI rats

Most of the changes that developed after tibial-NNI were similar when comparing nerves from hyperalgesic and non-hyperalgesic NNI rats. Data from tibial nerves are compared in Table 3. Ipsilesionally, only endoneurial area was different in hyperalgesic rats (22% greater, $p = 0.010$). The other data in Table 3 prove that this represents edema rather than increased numbers of axons or blood vessels. There was a trend towards more vasodilation among hyperalgesic rats (30% more, $p = 0.051$). Among contralesional tibial nerves, the only differences were vessel-wall thickness and microvessel luminal area. In contrast, no significant differences were identified in ipsilesional sural nerves of NNI-rats with versus without sural-zone hyperalgesia (Table 4). Within contralesional sural nerves, hyperalgesic NNI rats had more microvessels than non-hyperalgesic NNI rats.

3.4 Secondary evaluations of mast cells

Because of the unexpected finding of endoneurial axonopathy and inflammation within uninjured sural nerves as well as tibial nerves, we investigated whether or not the new distal endoneurial mast cells might have migrated from the proximal sciatic by performing a post-hoc analysis of the numbers of mast cells within common sciatic nerves dissected from rats' thighs, well proximal to the site of NNI. Five common sciatics from sham-operated control rats and 12 ipsilesional common sciatic nerves from NNI rats were available and adequate for analysis. Common sciatics from NNI rats had overall 43% fewer mast cells than sciatics from control rats, but because of high variability (range = 2 – 29), this was not significant ($p = 0.12$). Other trends included greater loss of mast cells from the epineurial (− 53%, $p = 0.17$) than endoneurial compartment (− 10%, $p = 0.80$), fewer proximal degranulated (−51%, $p = 0.07$) and granulated mast cells (−36%, $p = 0.36$). There were no evident mast-cell differences in rats with versus without hyperalgesia. The 12 contralesional common sciatics of NNI rats averaged 27% fewer mast cells ($p = 0.32$), but when comparing nerves from rats with ($n = 6$) vs. without ($n = 5$) tibial- or sural-territory hyperalgesia, non-hyperalgesic rats had 0% mast-cell reductions whereas hyperalgesic rats had 50% reduction from control values ($p = 0.09$).

4. Discussion

4.1 The endoneurial pathology of NNI reproduces that of CRPS-I

This detailed morphometric analysis of the effects of 18G tibial-nerve NNI on endoneurial cells distal to the injury identified changes not only in the injured nerve, but also in nearby uninjured sural nerves, and in uninjured tibial and sural nerves contralateral to the injury. Endoneurial microvasculopathy and inflammation were identified in addition to Wallerian axonal degeneration, a pattern common after larger nerve injuries including total axotomy and crush. Our study is limited by inability to detect stimulation-independent pain, the most important symptom of neuralgia/CRPS. There is still no validated method to detect chronic spontaneous pain in rodents (Mogil, 2009), largely because the behavioral correlates of acute pain extinguish over time. Some NNI rats occasionally licked or groomed their left hind paws, consistent with stimulus-independent sensations. Another limitation is inadequate analysis of post-operative recovery. Rats were dichotomized by their pain status at day 14, but we could not separate “recovered” from “never-affected” rats, partly because a rat could have recovered from one type of pain behavior while persisting with another. The phenotype is so complex that it is difficult to assemble phenotypically identical individuals for study. Similar difficulties apply to studies of patients. Future NNI experiments should start with even more rats for finer parsing of behavioral inclusion criteria. Thresholds for withdrawal from von Frey filaments were higher in these rats than in many other studies. As previously discussed (Siegel et al., 2007) this largely reflected use of the full range of von Frey monofilaments, because rats that did not withdraw were assigned the highest possible threshold, 1280 mN.

How does NNI pathology compare to findings in human patients? The current findings (axonopathy, microvasculopathy, and inflammation) are those that define human CRPS pathology extraneurally, in muscle and skin for instance (Albrecht et al., 2006; van der Laan et al., 1998). In the only primary study of endoneurial pathology, of nerves from 8 legs amputated from CRPS-I patients (van der Laan et al., 1998), injured and uninjured nerves were commingled and morphometry was only feasible for the sural nerves. This showed that 4/8 sural nerves had partial loss of myelinated and unmyelinated axons plus thickened endoneurial microvessel walls. Observation identified one subject with endoneurial edema and 3 with small epineurial infiltrates (uncharacterized). Thus, 18G tibial-NNI reasonably models the endoneurial pathology of CRPS-I.

How does NNI pathology compare to that from other rodent models? NNI is a diminutive of the widely used, spared-nerve-injury (SNI) model (Decosterd and Woolf, 2000). In SNI, tightly ligating and transecting the tibial and peroneal branches of the sciatic does not cause epidermal neurite losses in hindpaw skin innervated by the uninjured sural branch of the sciatic (Oaklander and Brown, 2004). Our finding that the smaller NNI lesion is more likely than SNI to cause sural axonopathy seems counter-intuitive. These differences suggest that partial nerve injuries (or injuries without proximal ligation) may be more likely to trigger spreading axonopathy than larger, total nerve lesions. Two other rat models also aim to reproduce the CRPS phenotype. The chronic post-ischemia pain (CPIP) model involves complete temporary occlusion of all blood-flow to one hindpaw. CPIP causes profound ischemia and microvascular dysfunction in distal muscles plus unspecified loss of cutaneous hindpaw epidermal innervation, at least during the first 7 days (Laferriere et al., 2008) but the chronic effects and the endoneurial pathology remain unreported. Tibia-fracture followed by limb casting, a clinically relevant injury, also causes CRPS-like sensory, vascular, and bone changes (Guo et al., 2004). The endoneurial pathology is unpublished but hindpaw epidermal innervation is unaltered (Wei et al., 2009), in contrast to NNI and CRPS-I (Oaklander et al., 2006).

4.2 Endoneurial microvessel changes after NNI: Potential relevance for CRPS

Microvascular abnormalities cause the distinctive phenotype of CRPS – edema, color and temperature changes – and contribute to underlying tissue ischemia, abnormal sweating, and bone dysregulation. This microvasculopathy has long been attributed to axonopathy, formerly to sympathetic overactivity. Current views have evolved, influenced by recognition that somatic innervation and circulating catecholamines also help regulate microvessel tone (Ruocco et al., 2002). The endoneurial microvessels of NNI rats also have complex changes. The wall thickening within ipsilesional tibial NNI nerves (and CRPS patients) is caused by basal-lamina accretion during repeated cycles of cell death and mitotic replacement (Vracko, 1974). Molecular mechanisms have only been studied in diabetes where they include hyperglycemia-induced upregulation of synthesis of type IV collagen, decreased expression of matrix metalloproteinases (MMP-2 and 3), and increased expression of tissue inhibitor of metalloproteinase (TIMP) (Tsilibary EC., 2003). Microvascular remodeling occurs early during Wallerian degeneration after nerve injury (Oaklander et al., 1987), breaching the blood-nerve barrier that maintains endoneurial homeostasis. Plasma extravasation then causes edema and intravascular hemoconcentration that promotes diapedesis and entrainment of hematogenous inflammatory cells. Because nerves have tough epineurial sheaths, endoneurial edema increases endoneurial pressure, potentially causing intrafascicular compartment syndrome that can further compromise circulation and axonopathy (Powell et al., 1979). Mast cell recruitment, also present in NNI, is a critical mediator (Enerback et al., 1965). So the feed-forward loops that link microvascular changes and inflammation can both be triggered by post-traumatic axonal degeneration, even when only a minority of axons is cut as in NNI. The contralesional thinning of endoneurial microvessel walls confirms that the ipsilesional wall thickening is a local rather than systemic effect, presumably a direct consequence of axonal injury. It is an unexplained new finding, potentially contributing to the plasma extravasation reported mirror-contralateral to unilateral nerve injuries (Kolston et al., 1991). The current findings further extend the number of “mirror” findings after unilateral nerve injury (Koltzenburg et al., 1999).

4.3 Endoneurial mast-cell changes after NNI: Potential relevance for CRPS

Mast cells often co-localize with unmyelinated axons, even forming synapse-like structures (Suzuki et al., 2004), and they localize near endoneurial microvessels, well-positioned to mediate the complex cellular interactions discussed here. Cross-talk via histamine, serotonin, neuropeptides, ATP, neurotrophins, proteinases, prostaglandins, leukotrienes, and cytokines (Stempelj and Ferjan, 2005; Schemann et al., 2005; Moriyama et al., 2005; Suzuki et al., 1999; Kakurai et al., 2006) creates feed-forward loops implicated in several neuro/vascular/inflammatory pain syndromes including CRPS, migraine, and interstitial cystitis (Huygen et al., 2004; Levy et al., 2007; Sant et al., 2007) Mobile mast cells are logical candidates to spread endoneurial changes away from the original injury. Despite the shared sciatic origin of the sural and tibial nerves, in NNI at least, spread of pathology to uninjured sural nerves was independent of mast-cell numbers. Given the trend towards increased mast cells in contralesional tibial nerves, a potential role for mast cells in contralesional changes should be more carefully examined.

4.4 Summary

NNI differs from other rat models of CRPS/post-traumatic neuralgia in causing a variable phenotype despite a highly standardized injury. Here we have extended knowledge of NNI to show that its endoneurial pathology models that of CRPS-I, further validating this model. The complex NNI model might help identify which post-axotomy changes are specifically associated with hyperalgesia —the current findings suggest that the inflammatory changes are more important than the number of axons cut. This conclusion meshes with those from recent data-mining studies linking CRPS-I to asthma and use of angiotensin-converting

enzymes (ACE) inhibitors, which augment substance P and bradykinin (de Mos et al., 2008; de Mos et al., 2009). Other recent human studies even implicate autoimmunity, with findings of anti-nerve antibodies and modest therapeutic benefit of intravenous immunoglobulin, a treatment for autoimmune neuropathy (Kohr et al., 2009; Goebel et al., 2010). Perhaps CRPS-I and post-NNI allodynia develop in individuals with greatest atopic response to nerve injuries?

Acknowledgments

Supported by the Public Health Service (NINDS NS42866, K24NS059892), the Reflex Sympathetic Dystrophy Association of America, and the National Organization for Rare Disorders. Presented in abstract form to the American Neurological Association and the Society for Neuroscience.

References

Albrecht PJ, Hines S, Eisenberg E, Pud D, Finlay DR, Connolly MK, Pare M, Davar G, Rice FL. Pathologic alterations of cutaneous innervation and vasculature in affected limbs from patients with complex regional pain syndrome. Pain. 2006; 120:244–266. [PubMed: 16427199]

Anseloni VC, Weng HR, Terayama R, Letizia D, Davis BJ, Ren K, Dubner R, Ennis M. Age-dependency of analgesia elicited by intraoral sucrose in acute and persistent pain models. Pain. 2002; 97:93–103. [PubMed: 12031783]

Basbaum AI, Gautron M, Jazat F, Mayes M, Guilbaud G. The spectrum of fiber loss in a model of neuropathic pain in the rat: an electron microscopic study. Pain. 1991; 47:359–367. [PubMed: 1664510]

Bennett GJ, Xie YK. A peripheral mononeuropathy in rat that produces disorders of pain sensation like those seen in man. Pain. 1988; 33:87–107. [PubMed: 2837713]

de Mos M, Huygen FJ, Dieleman JP, Koopman JS, Stricker BH, Sturkenboom MC. Medical history and the onset of complex regional pain syndrome (CRPS). Pain. 2008; 139:458–466. [PubMed: 18760877]

de Mos M, Huygen FJPM, Stricker BHC, Dieleman JP, Sturkenboom MCJM. The association between ACE inhibitors and the complex regional pain syndrome: Suggestions for a neuro-inflammatory pathogenesis of CRPS. Pain. 2009; 142:218–224. [PubMed: 19195784]

Decosterd I, Woolf CJ. Spared nerve injury: an animal model of persistent peripheral neuropathic pain. Pain. 2000; 87:149–158. [PubMed: 10924808]

Enerback L, Olsson Y, Sourander P. Mast cells in normal and sectioned peripheral nerve. Z Zellforsch. 1965; 66:596–608. [PubMed: 14342466]

Goebel A, Baranowski A, Maurer K, Ghiai A, McCabe C, Ambler G. Intravenous immunoglobulin treatment of the complex regional pain syndrome: a randomized trial. Ann Intern Med. 2010; 152:152–158. [PubMed: 20124231]

Guo TZ, Offley SC, Boyd EA, Jacobs CR, Kingery WS. Substance P signaling contributes to the vascular and nociceptive abnormalities observed in a tibial fracture rat model of complex regional pain syndrome type I. Pain. 2004; 108:95–107. [PubMed: 15109512]

Hargreaves K, Dubner R, Brown F, Flores C, Joris J. A new and sensitive method for measuring thermal nociception in cutaneous hyperalgesia. Pain. 1988; 32:77–88. [PubMed: 3340425]

Horowitz SH. Peripheral nerve injury and causalgia secondary to routine venipuncture. Neurology. 1994; 44:962–964. [PubMed: 8190306]

Huygen FJPM, Ramdhani N, van Toorenenbergen A, Klein J, Zijlstra FJ, Zijlstra FJ. Mast cells are involved in inflammatory reactions during Complex Regional Pain Syndrome type 1. Immunology Letters. 2004; 91:147–154. [PubMed: 15019283]

Kakurai M, Monteforte R, Suto H, Tsai M, Nakae S, Galli SJ. Mast cell-derived tumor necrosis factor can promote nerve fiber elongation in the skin during contact hypersensitivity in mice. Am J Pathol. 2006; 169:1713–1721. [PubMed: 17071594]

Kim SH, Chung JM. An experimental model for peripheral neuropathy produced by segmental spinal nerve ligation in the rat. Pain. 1992; 50:355–363. [PubMed: 1333581]

Kohr D, Tschernatsch M, Schmitz K, Singh P, Kaps M, Schafer KH, Diener M, Mathies J, Matz O, Kummer W, Maihofner C, Fritz T, Birklein F, Blaes F. Autoantibodies in complex regional pain syndrome bind to a differentiation-dependent neuronal surface autoantigen. Pain. 2009

Kolston J, Lisney SJ, Mulholland MN, Passant CD. Transneuronal effects triggered by saphenous nerve injury on one side of a rat are restricted to neurones of the contralateral, homologous nerve. Neurosci Lett. 1991; 130:187–189. [PubMed: 1795879]

Koltzenburg M, Wall PD, McMahon SB. Does the right side know what the left is doing? Trends Neurosci. 1999; 22:122–127. [PubMed: 10199637]

Lacroix-Fralish ML, Mogil JS. Progress in genetic studies of pain and analgesia. Annu Rev Pharmacol Toxicol. 2009; 49:97–121. [PubMed: 18834308]

Laferriere A, Millecamps M, Xanthos DN, Xiao WH, Siau C, de MM, Sachot C, Ragavendran JV, Huygen FJ, Bennett GJ, Coderre TJ. Cutaneous tactile allodynia associated with microvascular dysfunction in muscle. Mol Pain. 2008; 4:49. [PubMed: 18957097]

Lauria G, Cornblath DR, Johansson O, McArthur JC, Mellgren SI, Nolano M, Rosenberg N, Sommer C. EFNS guidelines on the use of skin biopsy in the diagnosis of peripheral neuropathy. Eur J Neurol. 2005; 12:747–758. [PubMed: 16190912]

Lee JW, Siegel SM, Oaklander AL. Effects of distal nerve injuries on dorsal-horn neurons and glia: Relationships between lesion size and mechanical hyperalgesia. Neuroscience. 2009; 158:904–914. [PubMed: 18992304]

Levy D, Burstein R, Kainz V, Jakubowski M, Strassman AM. Mast cell degranulation activates a pain pathway underlying migraine headache. Pain. 2007

Maves TJ, Pechman PS, Gebhart GF, Meller ST. Possible chemical contribution from chromic gut sutures produces disorders of pain sensation like those seen in man. Pain. 1993; 54:57–69. [PubMed: 8378104]

Mogil JS. Animal models of pain: progress and challenges. Nat Rev Neurosci. 2009; 10:283–294. [PubMed: 19259101]

Mogil JS, Lichtensteiger CA, Wilson SG. The effect of genotype on sensitivity to inflammatory nociception: characterization of resistant (A/J) and sensitive (C57BL/6J) inbred mouse strains. Pain. 1998; 76:115–125. [PubMed: 9696464]

Moriyama M, Takahiro S, Inoue H, Fukuyama S, Teranishi H, Kangawa K, Kano T, Yoshimura A, Kojima M. The neuropeptide neuromedin U promotes inflammation by direct activationof mast cells. The Journal of Experimental Medicine. 2005; 202:217–224. [PubMed: 16009716]

Oaklander AL, Brown JM. Unilateral nerve injury produces bilateral loss of distal innervation. Ann Neurol. 2004; 55:639–644. [PubMed: 15122703]

Oaklander AL, Miller MS, Spencer PS. Early changes in degenerating mouse sciatic nerve are associated with endothelial cells. Brain Res. 1987; 419:39–45. [PubMed: 2445427]

Oaklander AL, Rissmiller JG, Gelman LB, Zheng L, Chang Y, Gott R. Evidence of focal small-fiber axonal degeneration in complex regional pain syndrome-I (reflex sympathetic dystrophy). Pain. 2006; 120:235–243. [PubMed: 16427737]

Powell HC, Myers RR, Costello ML, Lampert PW. Endoneurial fluid pressure in wallerian degeneration. Ann Neurol. 1979; 5:550–557. [PubMed: 475350]

Ruocco I, Cuello AC, Parent A, Ribeiro-Da-Silva A. Skin blood vessels are simultaneously innervated by sensory, sympathetic, and parasympathetic fibers. J Comp Neurol. 2002; 448:323–336. [PubMed: 12115696]

Sant GR, Kempuraj D, Marchand JE, Theoharides TC. The mast cell in interstitial cystitis: Role in pathophysiology and pathogenesis. Urology. 2007; 69:S34–S40.

Schemann M, Michel K, Ceregrzyn M, Zeller F, Seidl S, Bischoff SC. Human mast cell mediator cocktail excites neurons in human and guinea-pig enteric nervous system. Neurogastroenterol Motil. 2005; 17:281–289. [PubMed: 15787948]

Seltzer Z, Dubner R, Shir Y. A novel behavioral model of neuropathic pain disorders produced in rats by partial sciatic nerve injury. Pain. 1990; 43:205–218. [PubMed: 1982347]

Siegel SM, Lee JW, Oaklander AL. Needlestick distal nerve injury in rats models symptoms of complex regional pain syndrome. Anesth Analg. 2007; 105:1820–1829. [PubMed: 18042888]

Stempelj M, Ferjan I. Signaling pathway in nerve growth factor induced histamine release from rat mast cells. Inflamm Res. 2005; 54:344–349. [PubMed: 16158335]

Suzuki A, Suzuki R, Furuno T, Teshima R, Nakanishi M. N-cadherin plays a role in the synapselike structures between mast cells and neurites. Biol Pharm Bull. 2004; 27:1891–1894. [PubMed: 15577201]

Suzuki R, Furuno T, McKay DM, Wolvers D, Teshima R, Nakanishi M, Bienenstock J. Direct neurite-mast cell communication in vitro occurs via the neuropeptide substance P. The Journal of Immunology. 1999; 163:2410–2415. [PubMed: 10452975]

Taiwo OB, Kovàcs KJ, Sperry LC, Larson AA. Naloxone-induced morphine withdrawal increases the number and degranulation of mast cells in the thalamus of the mouse. Neuropharmacology. 2004; 46:824–835. [PubMed: 15033342]

Tsilibary EC. Microvascular basement membranes in diabetes mellitus. J Pathol. 2003; 200:537–546. [PubMed: 12845621]

van der Laan L, ter Laak HJ, Gabreels-Festen A, Gabreels F, Goris RJ. Complex regional pain syndrome type I (RSD): pathology of skeletal muscle and peripheral nerve. Neurology. 1998; 51:20–25. [PubMed: 9674773]

Vracko R. Basal lamina layering in diabetes mellitus. Evidence for accelerated rate of cell death and cell regeneration. Diabetes. 1974; 23:94–104. [PubMed: 4590447]

Wei T, Li WW, Guo TZ, Zhao R, Wang L, Clark DJ, Oaklander AL, Schmelz M, Kingery WS. Post-junctional facilitation of Substance P signaling in a tibia fracture rat model of complex regional pain syndrome type I. Pain. 2009; 144:278–286. [PubMed: 19464118]

Zimmermann M. Ethical guidelines for investigations of experimental pain in conscious animals. Pain. 1983; 16:109–110. [PubMed: 6877845]

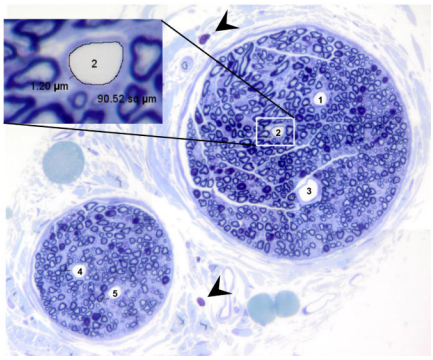

Figure 1.
Low-power 40× image of all fascicles of the ipsilesional sural nerve from a rat that underwent 18G tibial-NNI 14 days prior. It demonstrates that a minority of myelinated axons are undergoing Wallerian degeneration. Two epineurial and no endoneurial mast cells are visible (indicated by arrows). The inset illustrates the method of measuring area and wall thickness of endoneurial blood vessel number 2 of 5 counted in this nerve.

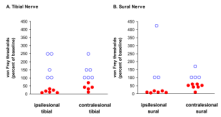

Figure 2.

Thresholds for hindpaw withdrawal from von Frey monofilaments at day 14 postoperative as compared to individual rats' preoperative baseline withdrawal thresholds (normalized to 100%). Panel A depicts values from tibial-innervated study sites; Panel B depicts values from sural-innervated study sites. Closed markers identify values below 100% (i.e., from rats with mechanical allodynia); open markers identify values at or above 100% (i.e., from non-allodynic rats). This analysis was performed in order to group tissues for pathological analysis (Section 3.3).

Table 1

Characterization of tibial nerves distal to 18G tibial needlestick-nerve-injury.

	Control nerves	Ipsilesional erves	*p*-value	Contralesional nerves	*p* -value
Intraepidermal neurite count	866 ± 62	599 ± 59	0.005*	805 ± 42	0.426
Endoneurial area (mm^2)	0.44 ± 0.02	0.57 ± 0.02	0.0002*	0.39 ± 0.02	0.063
Number of myelinated axons	4533 ± 105	3086 ± 127	0.0000*	4806 ± 175	0.200
Number of blood vessels	25.5 ± 2.1	25.9 ± 2.3	0.894	29.1 ± 1.7	0.206
Luminal area of each vessel (μm^2)	123.7 ± 7.4	142.4 ± 9.7	0.126	109.6 ± 6.3	0.147
Vessel wall thickness (μm)	2.01 ± 0.05	2.66 ± 0.09	0.0000*	1.74 ± 0.04	0.0001*
Endoneurial mast cells	2.9 ± 0.6	5.4 ± 0.6	0.010*	3.9 ± 0.8	0.316

Control nerves were from sham-operated rats (n = 10). Each group of experimental nerves contained 12 nerves. Data represent group mean ± SEM. Each comparison is to control nerves; asterisks identify p values significant after Bonferroni correction for multiple comparisons.

Table 2

Characterization of sural nerves in rats after 18G tibial needlestick-nerve-injury.

	Control nerves	Ipsilesional nerves	*p*-value	Contralesional nerves	*p* -value
Intraepidermal neurite count	956 ± 47	573 ± 88	0.001*	749 ± 72	0.027
Endoneurial area (mm^2)	0.057 ± 0.005	0.069 ± 0.009	0.224	0.070 ± 0.005	0.082
Number of myelinated axons	971 ± 65	697 ± 94	0.027	1060 ± 42	0.271
Number of blood vessels	4.6 ± 0.43	4.8 ± 0.7	0.853	5.0 ± 0.3	0.466
Luminal area of each vessel (μm^2)	64.92 ± 9.40	79.4 ± 10	0.302	120.1 ± 21.0	0.019*
Vessel wall thickness (μm)	1.38 ± 0.08	1.87 ± 0.15	0.005*	1.35 ± 0.07	0.812
Endoneurial mast cells	0.3 ± 0.2	0.8 ± 0.2	0.156	1.3 ± 0.5	0.076

Control nerves were from sham-operated rats (n = 10). Each group of experimental nerves contained 12 nerves. Data represent group mean ± SEM. Each comparison is to control nerves; asterisks identify p values significant after Bonferroni correction for multiple comparisons.

Table 3

Characterization of tibial nerves distal to 18G tibial needlestick-nerve-injury dichotomized by sensory testing results.

	Ipsilesional tibial			Contralesional tibial		
	hyperalgesic	**without hyperalgesia**	***p*-value**	**hyperalgesic**	**without hyperalgesia**	***p* -value**
Intraepidermal neurite count	601 ± 100	575 ± 74	0.838	858 ± 70	757 ± 59.5	0.308
Endoneurial area (mm^2)	0.61 ± 0.03	0.50 ± 0.02	0.010*	0.39 ± 0.03	0.41 ± 0.03	0.676
Number of myelinated axons	3040 ± 206	3115 ± 204	0.802	4865 ± 80	4574 ± 283	0.362
Number of blood vessels	27.8 ± 3.6	25.2 ± 3.1	0.594	31.2 ± 2.6	27.0 ± 2.7	0.289
Luminal area of each vessel (μm^2)	164.9 ± 15.3	126.7 ± 12.2	0.051	83.1 ± 6.3	129.4 ± 9.6	0.001*
Vessel wall thickness (μm)	2.5 ± 0.12	2.77 ± 0.13	0.161	1.49 ± 0.05	1.98 ± 0.07	0.000*
Endoneurial mast cells	6.0 ± 0.9	5.6 ± 0.7	0.731	3.6 ± 1.4	4.7 ± 0.8	0.543

Ipsilesional tibial nerves from NNI rats with (n = 6) versus without (n = 5) hyperalgesia, and contralesional tibial nerves from NNI rats with hyperalgesia (n = 5) versus without mechanical allodynia (n = 6). Data represent group mean ± SEM. Each comparison is between nerves from hyperalgesic and nonhyperalgesic rats;

asterisks identify p values significant after Bonferroni correction for multiple comparisons.

Table 4

Characterization of sural nerves from rats after 18G tibial needlestick-nerve-injury, dichotomized by sensory testing results.

	Ipsilesional sural			Contralesional sural		
	hyperalgesic	**without hyperalgesia**	***p*-value**	**hyperalgesic**	**without hyperalgesia**	***p* -value**
Intraepidermal neurite count	594 ± 93	326 ± 123	0.152	839 ± 100	560 ± 49	0.040
Endoneurial area (mm^2)	0.063 ± 0.013	0.081 ± 0.026	0.581	0.064 ± 0.008	0.082 ± 0.007	0.102
Number of myelinated axons	566 ± 142	801 ± 207	0.403	1029 ± 60	1117 ± 75	0.390
Number of blood vessels	3.3 ± 0.7	6.0 ± 1.5	0.214	5.6 ± 0.3	3.8 ± 0.3	0.001*
Luminal area of each vessel (μm^2)	72.0 ± 20.9	97.0 ± 19.0	0.381	100.6 ± 21.7	168.5 ± 61.5	0.312
Vessel wall thickness (μm)	2.36 ± 0.30	1.99 ± 0.25	0.355	1.34 ± 0.10	1.48 ± 0.12	0.408
Endoneurial mast cells	0.7 ± 0.2	0.7 ± 0.7	1.000	2.0 ± 0.8	0.3 ± 0.3	0.063

Ipsilesional sural nerves from NNI rats with (n = 6) versus without (n = 3) hyperalgesia, and contralesional sural nerves from NNI rats with hyperalgesia (n = 7) versus without mechanical allodynia (n = 4). Data represent group mean ± SEM. Each comparison is between nerves from hyperalgesic and nonhyperalgesic rats;

asterisks identify p values significant after Bonferroni correction for multiple comparisons.